

Observer-based Periodic Event-triggered and Self-triggered Boundary Control of a Class of Parabolic PDEs

Bhathiya Rathnayake, *Student Member, IEEE* and Mamadou Diagne, *Member, IEEE*

Abstract—This paper introduces the first observer-based periodic event-triggered control (PETC) and self-triggered control (STC) for boundary control of a class of parabolic PDEs using PDE backstepping control. We introduce techniques to convert a certain class of continuous-time event-triggered control into PETC and STC, eliminating the need for continuous monitoring of the event-triggering function. For the PETC, the event-triggering function requires only periodic evaluations to detect events, while the STC proactively computes the time of the next event right at the current event time using the system model and the continuously available measurements. For both strategies, the control input is updated exclusively at events and is maintained using a zero-order hold between events. We demonstrate that the closed-loop system is Zeno-free. We offer criteria for selecting an appropriate sampling period for the PETC and for determining the time until the next event under the STC. We prove the system’s global exponential convergence to zero in the spatial L^2 norm for both anti-collocated and collocated sensing and actuation under the PETC. For the STC, local exponential convergence to zero in the spatial L^2 norm for collocated sensing and actuation is proven. Simulations are provided to illustrate the theoretical claims.

Index Terms—Backstepping control design, event-triggered control, periodic event-triggered control, self-triggered control, reaction-diffusion systems.

I. INTRODUCTION

Event-triggered control (ETC) updates the control input based on events generated by a suitable event-triggering mechanism instead of at fixed intervals. This approach incorporates feedback into the control update tasks, allowing the control input to be updated aperiodically and only when necessary, based on the system’s states. Consequently, ETC reduces the frequency of control updates while maintaining a satisfactory level of performance in the closed-loop system [8].

ETC consists of a feedback control law that achieves desired closed-loop system properties and an event-triggered mechanism that specifies control input updates. A primary aim is avoiding Zeno behavior—infinite updates in a finite time—which is usually achieved by the careful design of the event-triggering mechanism so that it is endowed with a positive lower bound for the time between events, known as the minimal dwell-time. Research over the last decade

has expanded from ODEs [8] to those on PDEs, generating considerable advances (e.g. [3]–[5], [9], [11], [13], [14], [18]). Particularly, [13] and [14] significantly contribute to this work by introducing ETC for reaction-diffusion PDEs, with the former addressing an anti-collocated and the latter a collocated boundary sensing and actuation configuration.

A significant limitation of ETC for both ODEs and PDEs is the necessity for continuous-time monitoring of the triggering function to detect events, which is not ideal for digital implementations. These strategies are referred to as continuous-time ETC (CETC). To address this limitation, two alternative approaches have been developed:

- Periodic event-triggered control (PETC) which checks the event-triggering condition periodically and decides on control updates [6],
- Self-triggered control (STC) which proactively calculates the next event time at the current event time, using system states and the knowledge of the system’s dynamics [8].

Recent works on both PETC [2], [6], [7], [19] and STC [1], [10], [17], [20] of *ODE systems* have surfaced. However, their use in controlling *PDE plants* remains limited, with only a few papers addressing infinite-dimensional systems [15], [16]. Utilizing *semigroup theory*, [16] provides a *full-state feedback* PETC for infinite dimensional systems with unbounded control operators and point actuation whereas [15] provides a *full-state feedback* STC for infinite dimensional systems with *bounded control operators and spatially distributed actuation*.

The present contribution introduces the first *observer-based* PETC and STC for *boundary control* of a class of parabolic PDEs under Robin actuation using PDE backstepping approach.¹ Specifically, we present observer-based PETC designs when the boundary sensing and actuation are either collocated or anti-collocated and an observer-based STC design with collocated boundary sensing and actuation. Our designs are far from trivial and encompass all possible configurations of boundary sensing and actuation but anti-collocated sensing and actuation under STC.

The PETC results from a careful redesign of the continuous-time event-triggering function of the CETC [13], [14] to allow for periodic evaluation only. A novel periodic event triggering function is derived by finding an upper bound of the underlying continuous-time event-triggering function between two consecutive periodic evaluations. Subsequently, an explicit upper-bound of the allowable sampling period for periodic

¹The full-state feedback PETC was in part presented in [12].

B. Rathnayake is with the Department of Electrical and Computer Engineering, University of California San Diego, 9500 Gilman Dr, La Jolla, CA 92093. Email: brm222@ucsd.edu

M. Diagne is with the Department of Mechanical and Aerospace Engineering, University of California San Diego, 9500 Gilman Dr, La Jolla, CA 92093. Email: mdiagne@ucsd.edu

evaluation of the triggering function is obtained. Since the triggering function is evaluated periodically, and the control input is updated only when the function satisfies a certain condition upon evaluation, the Zeno behavior is inherently absent. Moreover, it is rigorously proven that the closed-loop system well-posedness and convergence under the CETC are preserved under the PETC. Specifically, the closed-loop signals under both CETC and PETC globally exponentially converges to zero in the spatial L^2 norm at the same rate.

The proposed STC consists of a uniformly and positively lower-bounded function that accepts several inputs involving the observer states, which, when evaluated at an event time, outputs the waiting time until the next event. The design of the positive function requires upper and lower bounds of constituent variables of the triggering function of the CETC. Since the function is uniformly and positively lower-bounded, the closed-loop system is Zeno-free by design. Moreover, the well-posedness of the closed-loop system under the STC is established. It is also proven that the closed-loop system under the STC exponentially converges to zero in the spatial L^2 norm locally at the same rate as its CETC counterpart.

Notation: By $C^0(A; \Omega)$, we denote the class of continuous functions on $A \subseteq \mathbb{R}^n$, which takes values in $\Omega \subseteq \mathbb{R}$. By $C^k(A; \Omega)$, where $k \geq 1$, we denote the class of continuous functions on A , which takes values in Ω and has continuous derivatives of order k . $L^2(0, 1)$ denotes the equivalence class of Lebesgue measurable functions $f : [0, 1] \rightarrow \mathbb{R}$ such that $\|f\| = (\int_0^1 |f(x)|^2)^{1/2} < \infty$. $H^1(0, 1)$ denotes the equivalence class of Lebesgue measurable functions $f : [0, 1] \rightarrow \mathbb{R}$ such that $\int_0^1 f^2(x)dx + \int_0^1 f_x^2(x)dx < \infty$. Let $u : [0, 1] \times \mathbb{R}_+ \rightarrow \mathbb{R}$ be given. $u[t]$ denotes the profile of u at certain $t \geq 0$, i.e., $(u[t])(x) = u(x, t)$, for all $x \in [0, 1]$. For an interval $J \subseteq \mathbb{R}_+$, the space $C^0(J; L^2(0, 1))$ is the space of continuous mappings $J \ni t \rightarrow u[t] \in L^2(0, 1)$.

II. PRELIMINARIES AND CONTINUOUS-TIME EVENT-TRIGGERED CONTROL (CETC)

Consider the following 1-D reaction-diffusion sampled-data boundary control system with constant coefficients:

$$u_t(x, t) = \varepsilon u_{xx}(x, t) + \lambda u(x, t), \text{ for } x \in (0, 1), \quad (1)$$

$$\theta_1 u_x(0, t) = -\theta_2 u(0, t), \quad (2)$$

$$u_x(1, t) = -qu(1, t) + U_j^\omega, \quad (3)$$

for all $t \in (t_j^\omega, t_{j+1}^\omega), j \in \mathbb{N}$, where $\theta_1 \theta_2 = 0$, $\theta_1 + \theta_2 = 1$, " ω " $\in \{“c”, “p”, “s”\}$, and $t_0^\omega = 0$. The sets $\{t_j^c\}_{j \in \mathbb{N}}$, $\{t_j^p\}_{j \in \mathbb{N}}$, and $\{t_j^s\}_{j \in \mathbb{N}}$ are event sequences from continuous-time event-triggering, periodic event-triggering, and self-triggering mechanisms. The initial condition is $u[0] \in L^2(0, 1)$, and the variables ε, λ, q are all positive. The inputs U_j^c, U_j^p , and U_j^s are CETC, PETC, and STC inputs, respectively, held constant for $t \in [t_j^\omega, t_{j+1}^\omega), j \in \mathbb{N}$. Note that θ_1 and θ_2 are either 0 or 1 and $\theta_1 \neq \theta_2$. The case $\theta_1 = 1, \theta_2 = 0$ leads to Neumann boundary condition at $x = 0$ whereas $\theta_1 = 0, \theta_2 = 1$ leads to Dirichlet boundary condition at $x = 0$.

In [13] and [14], the authors develop observers for the system (1)-(3) using boundary measurements. The former addresses anti-collocated boundary sensing and actuation with

$u(0, t)$ as the measurement, while the latter focuses on collocated boundary sensing and actuation with $u(1, t)$ as the measurement. These designs are presented below:

$$\begin{aligned} \hat{u}_t(x, t) &= \varepsilon \hat{u}_{xx}(x, t) + \lambda \hat{u}(x, t) \\ &\quad + p_1(x)(\theta_1 \tilde{u}(0, t) + \theta_2 \tilde{u}(1, t)), \text{ for } x \in (0, 1), \end{aligned} \quad (4)$$

$$\theta_1 \hat{u}_x(0, t) = -\theta_2 \hat{u}(0, t) + \theta_1 p_{10} \tilde{u}(0, t), \quad (5)$$

$$\hat{u}_x(1, t) = -q \hat{u}(1, t) + U_j^\omega + \theta_2 p_{10} \tilde{u}(1, t), \quad (6)$$

for all $t \in (t_j^\omega, t_{j+1}^\omega), j \in \mathbb{N}$, where $\hat{u}[0] \in L^2(0, 1)$ and

$$\tilde{u}(x, t) := u(x, t) - \hat{u}(x, t), \quad (7)$$

is the observer error. Here, the case $\theta_1 = 1, \theta_2 = 0$ results in anti-collocated sensing and actuation, and the case $\theta_1 = 0, \theta_2 = 1$ results in collocated sensing and actuation. The terms $p_1(x)$ and p_{10} are observer gains determined using the PDE backstepping technique equipped with the Volterra transformation:

$$\tilde{u}(x, t) = \tilde{w}(x, t) - \int_{\theta_2 x}^{\theta_1 x + \theta_2} P(x, y) \tilde{w}(y, t) dy, \quad (8)$$

with its inverse:

$$\tilde{w}(x, t) = \tilde{u}(x, t) + \int_{\theta_2 x}^{\theta_1 x + \theta_2} Q(x, y) \tilde{u}(y, t) dy, \quad (9)$$

for $0 \leq \theta_2 x + \theta_1 y \leq \theta_1 x + \theta_2 y \leq 1$. Details on the bounded observer gains $p_1(x)$ and p_{10} as well as the bounded gain kernels $P(x, y)$ and $Q(x, y)$ are found in [13] and [14].

The well-posedness of the closed-loop system (1)-(7) with piecewise constant inputs between two sampling instants is provided in the following proposition.

Proposition 1 ([13]). *For every $u[t_j^\omega], \hat{u}[t_j^\omega] \in L^2(0, 1)$, there exist unique solutions $u, \hat{u} : [t_j^\omega, t_{j+1}^\omega] \times [0, 1] \rightarrow \mathbb{R}$ between two time instants t_j^ω and t_{j+1}^ω such that $u, \hat{u} \in C^0([t_j^\omega, t_{j+1}^\omega]; L^2(0, 1)) \cap C^1((t_j^\omega, t_{j+1}^\omega) \times [0, 1])$ with $u[t], \hat{u}[t] \in C^2([0, 1])$ which satisfy (2),(3),(5),(6) for $t \in (t_j^\omega, t_{j+1}^\omega]$ and (1), (4) for $t \in (t_j^\omega, t_{j+1}^\omega), x \in (0, 1)$.*

Assumption 1. *The parameters q, λ , and ε satisfy the following relation:*

$$q > \frac{(\lambda + \theta_1 \varepsilon)}{2\varepsilon}. \quad (10)$$

Remark 1. Assumption 1 is required to avoid the use of the signal $u(1, t)$ in the nominal control law for which it is impossible to obtain a useful bound on its rate of change. Furthermore, It is worth mentioning that an eigenfunction expansion of the solution of (1)-(3) with $U_j^\omega = 0$ (zero input) shows that the system is unstable when $\lambda > \varepsilon \pi^2 / 4 \theta_1$, no matter what $q > 0$ (see Remark 1 in [13] and [14]). \square

In [13] and [14], the authors propose the following sampled-data boundary control law to be used in conjunction with event-triggering:

$$U_j^\omega := \int_0^1 k(y) \hat{u}(y, t_j^\omega) dy, \quad (11)$$

for $t \in [t_j^\omega, t_{j+1}^\omega), j \in \mathbb{N}$ where $k(y)$ is the control gain found using the PDE backstepping technique equipped with the Volterra transformation:

$$\hat{w}(x, t) = \hat{u}(x, t) - \int_0^x K(x, y) \hat{u}(y, t) dy, \quad (12)$$

with its inverse:

$$\hat{u}(x, t) = \hat{w}(x, t) + \int_0^x L(x, y) \hat{w}(y, t) dy, \quad (13)$$

for $0 \leq y \leq x \leq 1$. For further details on the bounded control gain $k(x)$ as well as the bounded gain kernels $K(x, y)$ and $L(x, y)$, the readers are referred to [13] and [14].

The sampled-data boundary control law (11) is derived through emulation. Specifically, this involves applying the underlying continuous-time control obtained via PDE backstepping in a sample-and-hold fashion between events. The difference between the sampled-data and the continuous-time control input, termed the input holding error, is defined by

$$d(t) := \int_0^1 k(y) (\hat{u}(y, t_j^\omega) - \hat{u}(y, t)) dy, \quad (14)$$

where $t \in [t_j^\omega, t_{j+1}^\omega)$ and $j \in \mathbb{N}$.

The authors of [13], [14] present a continuous-time event-triggering mechanism to determine the set of event times $\{t_j^c\}_{j \in \mathbb{N}}$ using $d(t)$ and a dynamic variable $m(t)$ via the following rule:

$$t_{j+1}^c = \inf \{t \in \mathbb{R}_+ | t > t_j^c, \Gamma^c(t) > 0, j \in \mathbb{N}\}, \quad (15)$$

with $t_0^c = 0$. The function $\Gamma^c(t)$ is defined as

$$\Gamma^c(t) := d^2(t) - \gamma m(t), \quad (16)$$

where $\gamma > 0$ is an event-trigger design parameter. The variable $m(t)$ evolves according to the ODE

$$\begin{aligned} \dot{m}(t) = & -\eta m(t) - \rho d^2(t) + \beta_1 \|\hat{u}[t]\|^2 + \beta_2 \hat{u}^2(1, t) \\ & + \theta_1 \beta_3 \tilde{u}^2(0, t) + \theta_2 \beta_3 \tilde{u}^2(1, t), \end{aligned} \quad (17)$$

valid for all $t \in (t_j^c, t_{j+1}^c), j \in \mathbb{N}$ with $m(t_0^c) = m(0) > 0$ and $m(t_j^{c-}) = m(t_j^c) = m(t_j^{c+})$, and $\eta, \rho, \beta_1, \beta_2, \beta_3 > 0$ are event-trigger parameters.

Assumption 2 (Event-trigger parameter selection). The parameters $\gamma, \eta > 0$ are design parameters, and $\beta_1, \beta_2, \beta_3 > 0$ are chosen such that

$$\beta_1 = \frac{\alpha_1}{\gamma(1-\sigma)}, \quad \beta_2 = \frac{\alpha_2}{\gamma(1-\sigma)}, \quad \beta_3 = \frac{\alpha_3}{\gamma(1-\sigma)}, \quad (18)$$

where $\sigma \in (0, 1)$ and

$$\alpha_1 = 4 \int_0^1 (\varepsilon k''(y) + \varepsilon k(1)k(y) + \lambda k(y)) dy, \quad (19)$$

$$\alpha_2 = 4(\varepsilon qk(1) + \varepsilon k'(1))^2, \quad (20)$$

$$\alpha_3 = 4 \left(\frac{\lambda(\theta_1 k(0) + \theta_2 k(1))}{2} + \int_0^1 k(y)p_1(y) dy \right)^2, \quad (21)$$

Subject to Assumption 1, the parameter $\rho > 0$ is chosen as

$$\rho = \frac{\varepsilon \kappa_1 B}{2}, \quad (22)$$

for $B, \kappa_1 > 0$ are chosen such that $B \left(\varepsilon \min \left\{ q - \frac{\lambda}{2\varepsilon} - \frac{\theta_1}{2}, \frac{1}{2} \right\} - \frac{\varepsilon}{2\kappa_1} - \frac{\lambda(5\theta_1 + 2\theta_2)}{8\kappa_2} - \frac{\|g\|^2}{\kappa_3} \right) - 2\beta_1 \tilde{L}^2 - 2\beta_2 - 4\beta_3 \tilde{L}^2 > 0$, for some $\kappa_2, \kappa_3 > 0$, where $g(x) = p_1(x) - \frac{\theta_1 \lambda}{2} K(x, 0) - \int_0^x K(x, y) p_1(y) dy$, $\tilde{L} = 1 + \left(\int_0^1 \int_0^x L^2(x, y) dy dx \right)^{1/2}$ and $\tilde{L} = \left(\int_0^1 L^2(1, y) dy \right)^{1/2}$ with $K(x, y)$ and $L(x, y)$ being the gain kernels of the backstepping transformations (12) and (13). Note from Assumption 1 that $q - \lambda/2\varepsilon - \theta_1/2 > 0$.

Theorem 1 (Results under CETC [13], [14]). Consider the CETC approach (11),(14)-(17) under Assumption 1, which generates a set of event-times $I^c = \{t_j^c\}_{j \in \mathbb{N}}$ with $t_0^c = 0$. It holds that

$$\Gamma^c(t) \leq 0 \text{ for all } t \in [t_j^c, t_{j+1}^c), j < j^{c*} \in \mathbb{N}, \quad (23)$$

where

$$j^{c*} = \inf \{i \in \mathbb{N} | t_i^c = \sup(I^c)\}. \quad (24)$$

Consequently, given appropriate choices for the event-trigger parameters $\gamma, \eta, \beta_1, \beta_2, \beta_3, \rho > 0$, the followings hold:

R1: The set of event-times I^c generates an increasing sequence for any $\eta, \gamma, \rho > 0$ and $\beta_1, \beta_2, \beta_3 > 0$ satisfying (18). Specifically, it holds that $t_{j+1}^c - t_j^c \geq \tau > 0, j \in \mathbb{N}$ where

$$\tau = \frac{1}{a} \ln \left(1 + \frac{\sigma a}{(1-\sigma)(a+\gamma\rho)} \right). \quad (25)$$

Here $\sigma \in (0, 1)$ appears in the relation (18), and

$$a = 1 + \rho_1 + \eta > 0, \quad (26)$$

where

$$\rho_1 = 4\varepsilon^2 k^2(1). \quad (27)$$

As $j \rightarrow \infty$, it follows that $t_j^c \rightarrow \infty$, thereby excluding Zeno behavior.

R2: For every $u[0], \hat{u}[0] \in L^2(0, 1)$, there exist unique solutions $u, \hat{u} : \mathbb{R}_+ \times [0, 1] \rightarrow \mathbb{R}$ such that $u, \hat{u} \in C^0(\mathbb{R}_+; L^2(0, 1) \cap C^1(J^c \times [0, 1]))$ with $u[t], \hat{u}[t] \in C^2([0, 1])$ which satisfy (2),(3),(5),(6) for all $t > 0$ and (1), (4) for all $t > 0, x \in (0, 1)$, where $J^c = \mathbb{R}_+ \setminus I^c$.

R3: The dynamic variable $m(t)$ governed by (17) with $m(0) > 0$ satisfies $m(t) > 0$ for all $t > 0$.

R4: As a result of R1-R3 and under Assumption 2, the closed-loop system (1)-(7) globally exponentially converges to zero in the spatial L^2 norm satisfying

$$\|u[t]\| + \|\hat{u}[t]\| \leq M e^{-\frac{b^*}{2}t} \sqrt{\|u[0]\|^2 + \|\hat{u}[0]\|^2 + m(0)}, \quad (28)$$

for all $t > 0$ and for some $M, b^* > 0$.

III. PERIODIC EVENT-TRIGGERED CONTROL (PETC) AND SELF-TRIGGERED CONTROL (STC)

A. Periodic Event-triggered Control (PETC)

In this subsection, we propose a PETC approach for the system described by equations (1)-(7) subject to Assumption 1. This approach is applicable under both anti-collocated ($\theta_1 = 1, \theta_2 = 0$) and collocated ($\theta_1 = 0, \theta_2 = 1$) sensing and actuation configurations. Our design draws from the CETC scheme in (11), (14)-(17). To implement this, we redesign the

triggering function $\Gamma^c(t)$, as specified in (16), into a new triggering function $\Gamma^p(t)$ which facilitates periodic evaluations. Furthermore, we determine a maximum allowable sampling period $h > 0$ for the periodic event-trigger. The proposed periodic event-triggering mechanism determines the set of event-times $\{t_j^p\}_{j \in \mathbb{N}}$ via the following rule:

$$t_{j+1}^p = \inf \{t \in \mathbb{R}_+ | t > t_j^p, \Gamma^p(t) > 0, t = nh, \\ h > 0, n \in \mathbb{N}\}, \quad (29)$$

with $t_0^p = 0$. Here, h is the sampling period selected as

$$0 < h \leq \tau, \quad (30)$$

where τ is given by (25) and $\Gamma^p(t)$ is given by

$$\Gamma^p(t) = (a + \gamma\rho)e^{ah}d^2(t) - \gamma\rho d^2(t) - \gamma am(t). \quad (31)$$

Here, $d(t)$ is given by (14) for $t \in [t_j^p, t_{j+1}^p), j \in \mathbb{N}$, $m(t)$ satisfies (17) for $t \in (t_j^p, t_{j+1}^p), j \in \mathbb{N}$, and a is given by (26).

Note that, under the continuous-time event-trigger (15)-(17), the triggering function $\Gamma^c(t)$ needs to be checked continuously to detect events. In contrast, with the periodic event-trigger (29)-(31), the triggering function $\Gamma^p(t)$ requires only periodic evaluations for event detection.

Theorem 2 (Results under PETC). *Consider the PETC approach (11),(29)-(31) under Assumption 1, which generates an increasing set of event-times $I^p = \{t_j^p\}_{j \in \mathbb{N}}$ with $t_0^p = 0$. For every $u[0], \hat{u}[0] \in L^2(0, 1)$, there exist unique solutions $u, \hat{u} : \mathbb{R}_+ \times [0, 1] \rightarrow \mathbb{R}$ such that $u, \hat{u} \in C^0(\mathbb{R}_+; L^2(0, 1) \cap C^1(J^p \times [0, 1]))$ with $u[t], \hat{u}[t] \in C^2([0, 1])$ which satisfy (2),(3),(5),(6) for all $t > 0$ and (1), (4) for all $t > 0, x \in (0, 1)$, where $J^p = \mathbb{R}_+ \setminus I^p$. Given appropriate choices for the event-trigger parameters $\gamma, \eta, \beta_1, \beta_2, \beta_3, \rho > 0$, the followings hold:*

- R1: For any $\eta, \gamma, \rho > 0$ and $\beta_1, \beta_2, \beta_3 > 0$ satisfying (18), the function $\Gamma^c(t)$ given by (16) satisfies $\Gamma^c(t) \leq 0$ for all $t > 0$ along the solution of (1)-(7),(11),(14),(17),(29)-(31).
- R2: The dynamic variable $m(t)$ governed by (17) with $m(0) > 0$ satisfies $m(t) > 0$ for all $t > 0$ along the solution of (1)-(7),(11),(14),(29)-(31).
- R3: Under Assumption 2, the closed-loop system (1)-(7) globally exponentially converges to zero in the spatial L^2 norm satisfying (28).

The complete proof is provided in the Appendix-A.

B. Self-triggered Control (STC)

In this subsection, we propose an STC approach for the system described by equations (1)-(7) under collocated sensing and actuation configuration ($\theta_1 = 0, \theta_2 = 1$) and subject to Assumption 1. Furthermore, we make the following assumption on initial data.

Assumption 3. *The initial conditions of the plant (1)-(3) and the observer (4)-(6) with $\theta_1 = 0, \theta_2 = 1$ satisfy $u[0], \hat{u}[0] \in H^1(0, 1)$. Further, for some known constants $\Psi_1, \Psi_2 > 0$, it holds that*

$$\|u[0]\| \leq \Psi_1, \text{ and } \|u_x[0]\| \leq \Psi_2. \quad (32)$$

Our design draws from the CETC scheme in (11), (14)-(17). We propose a function $G(\cdot, \cdot)$ that is uniformly positive

and lower-bounded, and which depends on the observer states. When this function is evaluated at the current event time, it yields the waiting time until the subsequent event. The proposed self-triggering mechanism determines the sequence of event times $\{t_j^s\}_{j \in \mathbb{N}}$ according to the following rule:

$$t_{j+1}^s = t_j^s + G(\|\hat{u}[t_j^s]\|, m(t_j^s)), \quad (33)$$

with $t_0^s = 0$ where $G(\cdot, \cdot) > 0$ is a uniformly and positively lower-bounded function

$$G(\|\hat{u}[t_j^s]\|, m(t_j^s), t_j^s) \\ := \max \left\{ \tau, \frac{1}{2\varrho + \eta} \ln \left(\frac{\gamma m(t_j^s) + \frac{\gamma \rho H(t_j^s)}{2\varrho + \eta}}{H(t_j^s) + \frac{\gamma \rho H(t_j^s)}{2\varrho + \eta}} \right) \right\}, \quad (34)$$

In (34), $H(t)$ is given by

$$H(t) = 2\|k\|^2 \left(2\|\hat{u}[t]\|^2 + \frac{\varepsilon^2 \|k\|^2}{\lambda \varrho} \|\hat{u}[t]\|^2 + \frac{(\Psi_0^*)^2 e^{-2\sigma^* t}}{\varrho} \right), \quad (35)$$

where

$$\varrho = \lambda + \frac{\|p_1\|^2}{2}, \quad \sigma^* \in \left(0, \frac{\varepsilon \pi^2}{4} \right], \quad (36)$$

and Ψ_0^* is given by

$$\Psi_0^* = \frac{1}{\sqrt{2}} \left(((M_1 + 1)\Omega_1 + \Omega_2) \Psi_1 + \Psi_2 \right. \\ \left. + ((M_1 + 1)\Omega_1 + \Omega_2) \|\hat{u}[0]\| + \|\hat{u}_x[0]\| \right) \\ \times \sqrt{\left(\frac{\varepsilon^2 p_{10}^2}{\lambda} + \frac{1}{2} \right)}. \quad (37)$$

In (37), $\Psi_1, \Psi_2 > 0$ are the known bounds of $\|u[0]\|$ and $\|u_x[0]\|$, respectively, as stated in Assumption 3 and M_1, Ω_1, Ω_2 are given by

$$M_1 = 2q + \frac{2\varepsilon q^2}{\varepsilon \pi^2 / 4 + 2\varepsilon q - \sigma^*}, \quad (38)$$

$$\Omega_1 = 1 + \sqrt{\int_0^1 \int_x^1 Q^2(x, y) dy dx}, \quad (39)$$

and

$$\Omega_2 = \max_{x \in [0, 1]} |Q(x, x)| + \sqrt{\int_0^1 \int_x^1 Q_x^2(x, y) dy dx}, \quad (40)$$

where $Q(x, y)$ is the gain kernel of the inverse backstepping transformation (9). Referring to [14], one can show that $\max_{x \in [0, 1]} |Q(x, x)| = \lambda/2\varepsilon$.

Theorem 3 (Results under STC). *Consider the STC approach (11),(33)-(40) under Assumptions 1 and 3, which generates an increasing set of event-times $I^s = \{t_j^s\}_{j \in \mathbb{N}}$ with $t_0^s = 0$. For every $u[0], \hat{u}[0] \in L^2(0, 1)$, there exist unique solutions $u, \hat{u} : \mathbb{R}_+ \times [0, 1] \rightarrow \mathbb{R}$ such that $u, \hat{u} \in C^0(\mathbb{R}_+; L^2(0, 1) \cap C^1(J^s \times [0, 1]))$ with $u[t], \hat{u}[t] \in C^2([0, 1])$ which satisfy (2),(3),(5),(6) for all $t > 0$ and (1), (4) for all $t > 0, x \in (0, 1)$, where $J^s = \mathbb{R}_+ \setminus I^s$. Given appropriate choices for the event-trigger parameters $\gamma, \eta, \beta_1, \beta_2, \beta_3, \rho > 0$, the followings hold:*

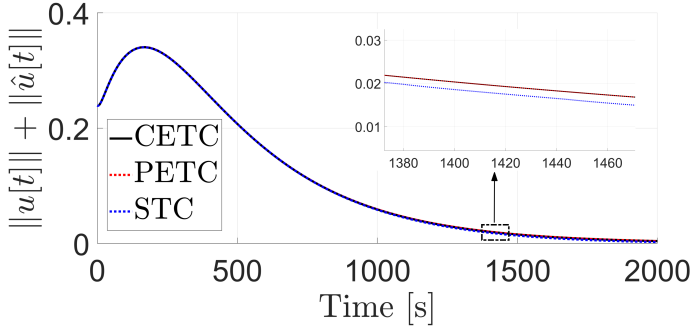


Fig. 1: Evolution of $\|u[t]\| + \|\hat{u}[t]\|$

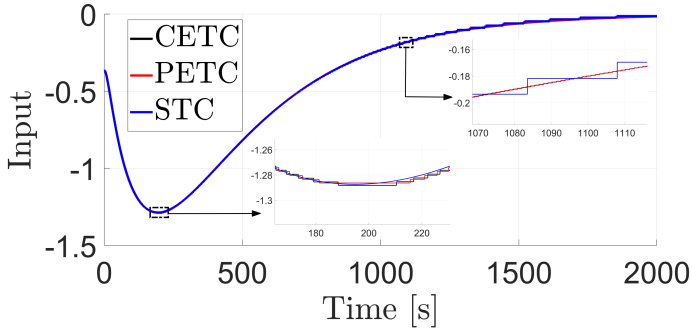


Fig. 2: Boundary control inputs.

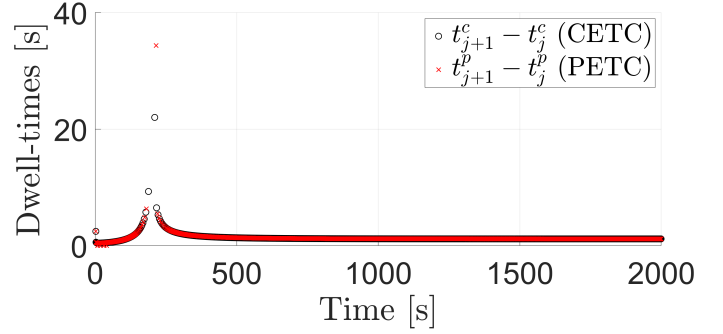


Fig. 3: Dwell-times under CETC and PETC.

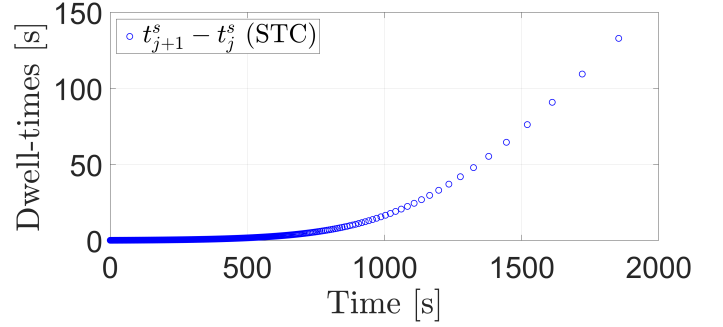


Fig. 4: Dwell-times under STC.

- R1: For any $\eta, \gamma, \rho > 0$ and $\beta_1, \beta_2, \beta_3 > 0$ satisfying (18), the function $\Gamma^c(t)$ given by (16) satisfies $\Gamma^c(t) \leq 0$ for all $t > 0$ along the solution of (1)-(7),(11),(14),(17),(33)-(40).
- R2: The dynamic variable $m(t)$ governed by (17) with $m(0) > 0$ satisfies $m(t) > 0$ for all $t > 0$ along the solution of (1)-(7),(11),(14),(33)-(40).
- R3: Under Assumption 2, the closed-loop system (1)-(7) locally exponentially converges to zero in the spatial L^2 norm satisfying (28).

The complete proof is provided in the Appendix-B.

Remark 2. When $u[0]$ and $\hat{u}[0]$ are in $H^1(0, 1)$, they are also in $L^2(0, 1)$. As a result, the well-posedness of the closed-loop system (1)-(6), in the context of Theorem 3, directly follows from Proposition 1. The solution is constructed iteratively between consecutive event times.

IV. NUMERICAL SIMULATIONS

We consider an open loop unstable reaction-diffusion PDE with $\varepsilon = 0.001, \lambda = 0.01, q = 5.1, \theta_1 = 0, \theta_2 = 1$ and the initial conditions $u[0] = 5x^2(x-1)^2$ and $\hat{u}[0] = x^2(x-1)^2$. For numerical simulations, both the plant and the observer are discretized with a uniform step size of $\Delta x = 0.005$ for the space variable. The discretization with respect to time is done using the implicit Euler scheme with step size $\Delta t = 0.001s$. The parameters for the CETC and PETC are chosen as follows: $m(0) = 10^{-4}, \gamma = 1, \eta = 1$ and $\sigma = 0.9$. We can compute using (19)-(21) that $\alpha_1 = 0.021; \alpha_2 = 0.0131; \alpha_3 = 0.7971$. Therefore, from (18), we can obtain $\beta_1 = 0.2095; \beta_2 = 0.1309; \beta_3 = 7.9706$. Let us choose $\kappa_1 = 25$ and $B =$

7.7304×10^4 , and then, from (22), we can obtain $\rho = 966.3$. The parameters for the STC are chosen as follows: $m(0) = 10^{-4}, \gamma = 10^{12}, \eta = 10^{-6}, \sigma = 0.9, \Psi_1 = 0.1992, \Psi_2 = 0.6901$, and $\sigma^* = \varepsilon\pi^2/4$. Therefore, from (18), we can obtain $\beta_1 = 2.095 \times 10^{-13}; \beta_2 = 1.31 \times 10^{-13}; \beta_3 = 7.9706 \times 10^{-12}$. Let us choose $\kappa_1 = 25$ and $B = 7.7304 \times 10^{-8}$, and then, from (22), we can obtain $\rho = 9.6630 \times 10^{-10}$. For all the strategies, the minimal dwell-time τ calculated using (25) is $0.009s$. For the PETC, we choose the sampling period for evaluating the triggering function as $h = 0.009s$.

Fig. 1 shows the response of the closed-loop system under CETC, PETC, and STC. Fig. 2 shows the corresponding control inputs. We can observe that the spatial L^2 norm of the closed-loop signals under CETC, PETC, and STC converge to zero at roughly similar rates, despite PETC and STC not requiring continuous monitoring of a triggering function, as opposed to CETC. In Figs. 3 and 4, we can observe that both CETC and PETC trigger events at similar rates, whereas STC triggers more frequent events than CETC and PETC initially. However, as the closed-loop system approaches the equilibrium, the frequency of events under STC significantly becomes lower than those under CETC and PETC.

V. CONCLUSION

In this paper, we have proposed novel observer-based PETC and STC strategies for a class of reaction-diffusion systems with Robin boundary actuation. Specifically, we have presented observer-based PETC designs when the sensing and actuation are either collocated or anti-collocated and an observer-based STC design with collocated sensing and actuation. The key idea of the developed methods is the transformation

of a class of continuous-time dynamic event-triggers which require continuous monitoring to periodic event-triggers and self-triggers. For the PETC, we have obtained an explicit upper-bound of the allowable sampling period of the periodic event-trigger. For the STC, we have designed a positively lower-bounded function which, when evaluated at the time of an event, outputs the waiting time until the next event. The well-posedness of the closed-loop system under both PETC and STC has been proven for all cases. Further, we have proven that the global exponential convergence to zero in the spatial L^2 norm under the CETC is preserved under the proposed PETC. The STC ensures that the closed-loop system exponentially converges to zero in the spatial L^2 norm locally at a comparable rate to its CETC counterpart. The conducted numerical simulation has illustrated the validity of the theoretical developments.

APPENDIX

A. Proof of Theorem 2

The well-posedness of the closed-loop system (1)-(6) under the PETC, in the sense of Theorem 2, directly follows from Proposition 1. The solution is constructed iteratively between consecutive event times. To streamline the rest of the proof of Theorem 2, we first present Lemmas 1 and 2.

Lemma 1. *Consider the PETC approach (11),(29)-(31) which generates an increasing set of event-times $I^p = \{t_j^p\}_{j \in \mathbb{N}}$ with $t_0^p = 0$. For $d(t)$ given by (14), it holds that*

$$\begin{aligned} d^2(t) &\leq \rho_1 d^2(t) + \alpha_1 \|\hat{u}[t]\|^2 + \alpha_2 \hat{u}^2(1, t) + \theta_1 \alpha_3 \tilde{u}^2(0, t) \\ &\quad + \theta_2 \alpha_3 \tilde{u}^2(1, t), \end{aligned} \quad (41)$$

along the solution of (1)-(7) for all $t \in (nh, (n+1)h)$ and any $n \in [t_j^p/h, t_{j+1}^p/h) \subset \mathbb{N}$. Here $\alpha_1, \alpha_2, \alpha_3, \rho_1 > 0$ are given by (19)-(21),(27), respectively.

The proof is very similar to that of Lemma 2 in [13], and hence omitted.

Lemma 2. *Consider the PETC approach (11),(29)-(31) under Assumption 1, which generates an increasing set of event-times $\{t_j^p\}_{j \in \mathbb{N}}$ with $t_0^p = 0$. For any $\eta, \gamma, \rho > 0$ and $\beta_1, \beta_2, \beta_3 > 0$ satisfying (18), $\Gamma^c(t)$ given by (16) satisfies*

$$\begin{aligned} \Gamma^c(t) &\leq \frac{1}{a} \left((a + \gamma\rho) d^2(nh) e^{a(t-nh)} - \gamma\rho d^2(nh) \right. \\ &\quad \left. - \gamma a m(nh) \right) e^{-\eta(t-nh)}, \end{aligned} \quad (42)$$

where a is given by (26), and h is the sampling period chosen as in (30), along the solution of (1)-(7),(11),(14),(17),(29)-(31) for all $t \in [nh, (n+1)h)$ and any $n \in [t_j^p/h, t_{j+1}^p/h) \subset \mathbb{N}$.

Proof of Lemma 2. Taking the time derivative of (16) in $t \in (nh, (n+1)h)$ and $n \in [t_j^p/h, t_{j+1}^p/h) \subset \mathbb{N}$, using Young's inequality, the relation (41), the dynamics of $m(t)$ given by (17), and (16) to substitute for $d^2(t)$, we can show that

$$\begin{aligned} \dot{\Gamma}^c(t) &\leq (1 + \rho_1 + \gamma\rho) \Gamma^c(t) + \gamma(a + \gamma\rho) m(t) \\ &\quad - (\gamma\beta_1 - \alpha_1) \|\hat{u}[t]\|^2 - (\gamma\beta_2 - \alpha_2) \hat{u}^2(1, t) \\ &\quad - (\gamma\beta_3 - \alpha_3) (\theta_1 \tilde{u}^2(0, t) + \theta_2 \tilde{u}^2(1, t)). \end{aligned}$$

Noting that both sides of this inequality are well-behaved in $t \in (nh, (n+1)h)$ and $n \in [t_j^p/h, t_{j+1}^p/h) \subset \mathbb{N}$, we can assert,

there exists a non-negative function $\iota(t) \in C^0((t_j^p, t_{j+1}^p); \mathbb{R}_+)$ such that

$$\begin{aligned} \dot{\Gamma}^c(t) &= (1 + \rho_1 + \gamma\rho) \Gamma^c(t) + \gamma(a + \gamma\rho) m(t) \\ &\quad - (\gamma\beta_1 - \alpha_1) \|\hat{u}[t]\|^2 - (\gamma\beta_2 - \alpha_2) \hat{u}^2(1, t) \\ &\quad - (\gamma\beta_3 - \alpha_3) (\theta_1 \tilde{u}^2(0, t) + \theta_2 \tilde{u}^2(1, t)) - \iota(t), \end{aligned} \quad (43)$$

for all $t \in (nh, (n+1)h)$ and $n \in [t_j^p/h, t_{j+1}^p/h) \subset \mathbb{N}$. Furthermore, using (16) to substitute for $d^2(t)$, we can rewrite the dynamics of $m(t)$ as

$$\begin{aligned} \dot{m}(t) &= -\rho \Gamma^c(t) - (\gamma\rho + \eta) m(t) + \beta_1 \|\hat{u}[t]\|^2 \\ &\quad + \beta_2 \hat{u}^2(1, t) + \beta_3 (\theta_1 \tilde{u}^2(0, t) + \theta_2 \tilde{u}^2(1, t)), \end{aligned} \quad (44)$$

for $t \in (nh, (n+1)h)$ and $n \in [t_j^p/h, t_{j+1}^p/h) \subset \mathbb{N}$. Then, concatenating the equations (43) and (44), we can obtain the following ODE system

$$\dot{z}(t) = Az(t) + v(t), \quad (45)$$

where

$$\begin{aligned} z(t) &= \begin{bmatrix} \Gamma^c(t) \\ m(t) \end{bmatrix}, \quad A = \begin{bmatrix} 1 + \rho_1 + \gamma\rho & \gamma(a + \gamma\rho) \\ -\rho & -(\gamma\rho + \eta) \end{bmatrix}, \\ v(t) &= \begin{bmatrix} \left(-(\gamma\beta_1 - \alpha_1) \|\hat{u}[t]\|^2 - (\gamma\beta_2 - \alpha_2) \hat{u}^2(1, t) \right. \\ \left. - (\gamma\beta_3 - \alpha_3) (\theta_1 \tilde{u}^2(0, t) + \theta_2 \tilde{u}^2(1, t)) - \iota(t) \right) \\ \left(\beta_1 \|\hat{u}[t]\|^2 + \beta_2 \hat{u}^2(1, t) \right. \\ \left. + \beta_3 (\theta_1 \tilde{u}^2(0, t) + \theta_2 \tilde{u}^2(1, t)) \right) \end{bmatrix}. \end{aligned}$$

From (45), we derive that

$$z(t) = e^{A(t-nh)} z(nh) + \int_{nh}^t e^{A(t-\xi)} v(\xi) d\xi,$$

for all $t \in [nh, (n+1)h)$ and $n \in [t_j^p/h, t_{j+1}^p/h) \subset \mathbb{N}$, using which we obtain

$$\Gamma^c(t) = C e^{A(t-nh)} z(nh) + \int_{nh}^t C e^{A(t-\xi)} v(\xi) d\xi,$$

where $C = [1 \ 0]$. The matrix A has two distinct eigenvalues $-\eta$ and $1 + \rho_1$. Therefore, using the matrix diagonalization of A and after some simplifications, it can be shown that

$$\begin{aligned} C e^{A(t-\xi)} v(\xi) &= -((\gamma\beta_1 - \alpha_1) g_1(t - \xi) - \beta_1 g_2(t - \xi)) \|\hat{u}[\xi]\|^2 \\ &\quad - ((\gamma\beta_2 - \alpha_2) g_1(t - \xi) - \beta_2 g_2(t - \xi)) \hat{u}^2(1, \xi) \\ &\quad - \theta_1 ((\gamma\beta_3 - \alpha_3) g_1(t - \xi) - \beta_3 g_2(t - \xi)) \tilde{u}^2(0, t) \\ &\quad - \theta_2 ((\gamma\beta_3 - \alpha_3) g_1(t - \xi) - \beta_3 g_2(t - \xi)) \tilde{u}^2(1, t) \\ &\quad - g_1(t - \xi) \iota(\xi), \end{aligned}$$

where

$$g_1(t) = \frac{1}{a} (-\gamma\rho + (a + \gamma\rho) e^{at}) e^{-\eta t},$$

and

$$g_2(t) = \frac{\gamma(a + \gamma\rho)}{a} (-1 + e^{at}) e^{-\eta t}.$$

We can easily observe that $g_1(t) > 0$ for all $t \geq 0$. Furthermore, noting that $\gamma\beta_i/\alpha_i = 1/(1 - \sigma)$, $i = 1, 2, 3$ from (18), and recalling (25), we can show that

$$\begin{aligned} &(\gamma\beta_i - \alpha_i) g_1(t - \xi) - \beta_i g_2(t - \xi) \\ &= \frac{\alpha_i(a + \gamma\rho)}{a} \left(1 + \frac{\sigma a}{(1 - \sigma)(a + \gamma\rho)} - e^{a(t-\xi)} \right) e^{-\eta(t-\xi)} \\ &= \frac{\alpha_i(a + \gamma\rho)}{a} \left(e^{a\tau} - e^{a(t-\xi)} \right) e^{-\eta(t-\xi)}, \end{aligned}$$

for $i = 1, 2, 3$. As $nh \leq \xi \leq t < (n+1)h$, and $h \leq \tau$, we have that $(\gamma\beta_i - \alpha_i)g_1(t - \xi) - \beta_i g_2(t - \xi) > 0$ for $i = 1, 2, 3$. Thus, we can argue that $Ce^{A(t-\xi)}v(\xi) \leq 0$ for all t, ξ such that $nh \leq \xi \leq t < (n+1)h$, and $n \in [t_j^p/h, t_{j+1}^p/h) \subset \mathbb{N}$. Considering this, it can be derived for $t \in [nh, (n+1)h)$ that

$$\begin{aligned} \Gamma^c(t) &\leq Ce^{A(t-nh)}z(nh) \\ &\leq g_1(t - nh)\Gamma^c(nh) + g_2(t - nh)m(nh) \\ &\leq \frac{1}{a} \left(-\gamma(a + \gamma\rho)m(nh) - \gamma\rho\Gamma^c(nh) \right. \\ &\quad \left. + (a + \gamma\rho)(\Gamma^c(nh) + \gamma m(nh))e^{a(t-nh)} \right) e^{-\eta(t-nh)}. \end{aligned}$$

By substituting for $\Gamma^c(nh)$ using (16), we obtain the inequality (42) that is valid for $t \in [nh, (n+1)h)$. This completes the proof of Lemma 2 \blacksquare

Now let us continue with the proof of Theorem 2. Assume that an event has triggered at $t = t_j^p$ and $m(t_j^p) > 0$. Then, let us analyze the behavior of $\Gamma^c(t)$ and $m(t)$ in $t \in [t_j^p, t_{j+1}^p)$ along the solution of (1)-(7),(11),(14),(17),(29)-(31). After the event at $t = t_j^p$, the control law is updated. Thus, we have from (16) that $\Gamma^c(t_j^p) = -\gamma m(t_j^p) < 0$. Consequently, $\Gamma^c(t)$ will at least remain non-positive until $t = t_j^p + \tau$ where τ is the minimal dwell-time given by (25) (see R1 of Theorem 1). Thus, $\Gamma^c(t)$ will definitely remain non-positive in $t \in [t_j^p, t_j^p + h)$ as $h \leq \tau$. However, at each $t = nh, n > 0$, the periodic event-trigger given by (29)-(31) is evaluated, and only if $\Gamma^p(nh) > 0$ that an event is triggered, and the control input is updated. If $\Gamma^p(nh) \leq 0$, then an update would not be required as $\Gamma^c(t)$ will be non-positive due to the relation (42) (Note that the right hand side of (42) is definitely non-positive when $\Gamma^p(nh) \leq 0$). Thus, $\Gamma^c(t)$ will in fact remain non-positive at least until $t = t_{j+1}^p$ where $\Gamma^p(t_{j+1}^p) > 0$. As $\Gamma^c(t) \leq 0$ for $t \in [t_j^p, t_{j+1}^p)$, we can write from (16) that $d^2(t) \leq \gamma m(t)$ for $t \in [t_j^p, t_{j+1}^p)$. Then, considering the dynamics of $m(t)$ given by (17), we get $\dot{m}(t) \geq -(\eta + \gamma\rho)m(t)$ for $t \in (t_j^p, t_{j+1}^p)$, which leads to $m(t) \geq e^{-(\eta + \gamma\rho)(t-t_j^p)}m(t_j^p) > 0$ for $t \in [t_j^p, t_{j+1}^p)$. The time continuity of $m(t)$ leads to $m(t_{j+1}^p) = m(t_{j+1}^p) > 0$. Therefore, after the control input has been updated at $t = t_{j+1}^p$, we obtain the equality $\Gamma^c(t_{j+1}^p) = -\gamma m(t_{j+1}^p) < 0$. In a similar way, we can analyze the behavior of $\Gamma^c(t)$ and $m(t)$ in all $t \in [t_j^p, t_{j+1}^p)$ for any $j \in \mathbb{N}$ starting from the first event at $t_0^p = 0$ where $m(0) > 0$ to prove that $\Gamma^c(t) \leq 0$ for all $t \in [t_j^p, t_{j+1}^p), j \in \mathbb{N}$ and $m(t) > 0$ for all $t > 0$. Thus, the global L^2 -exponential convergence of the closed-loop system to zero satisfying the estimate (28) follows from R4 of Theorem 1. This completes the proof of Theorem 2. \blacksquare

B. Proof of Theorem 3

The well-posedness of the closed-loop system (1)-(6) with $\theta_1 = 0, \theta_2 = 1$ under the STC is discussed in Remark 2. To streamline the proof of Theorem 3, we first present Lemma 3. **Lemma 3.** Consider the STC approach (33)-(40) under Assumptions 1 and 3, which generates an increasing set of event times $\{t_j^s\}_{j \in \mathbb{N}}$ with $t_j^s = 0$. Then, for the error $d(t)$ given by (14) and $m(t)$ governed by (17), the followings hold:

$$d^2(t) \leq H(t_j^s)e^{2\varrho(t-t_j^s)}, \quad (46)$$

and

$$m(t) \geq m(t_j^s)e^{-\eta(t-t_j^s)} - \frac{\rho H(t_j^s)}{2\varrho + \eta} e^{-\eta(t-t_j^s)} (e^{(2\varrho + \eta)(t-t_j^s)} - 1), \quad (47)$$

for all $t \in [t_j^s, t_{j+1}^s), j \in \mathbb{N}$ along the solution of (1)-(7), where $H(t)$ and ϱ are given by (35) and (36), respectively.

Proof of Lemma 3. Consider the positive definite function

$$V = \frac{1}{2} \int_0^1 \hat{u}^2(x, t) dx. \quad (48)$$

Taking its time derivative along the solution (4)-(6) and using Young's inequality and Cauchy Schwarz inequality, we can show that

$$\begin{aligned} \dot{V} &\leq -\varepsilon q \hat{u}^2(1, t) - \varepsilon \|\hat{u}_x[t]\|^2 + \lambda \|\hat{u}[t]\|^2 + \frac{\varepsilon h_1}{2} \hat{u}^2(1, t) \\ &\quad + \frac{\varepsilon}{2h_1} (U_j^s)^2 + \frac{\varepsilon p_{10}}{2h_2} \hat{u}^2(1, t) + \frac{\varepsilon p_{10} h_2}{2} \hat{u}^2(1, t) \\ &\quad + \frac{1}{2h_3} \hat{u}^2(1, t) + \frac{\|p_1\|^2 h_3}{2} \|\hat{u}[t]\|^2, \end{aligned}$$

for $t \in (t_j^s, t_{j+1}^s), j \in \mathbb{N}$ and some $h_1, h_2, h_3 > 0$. Let us select $h_1 = \frac{\lambda}{2\varepsilon}, h_2 = \frac{2\varepsilon p_{10}}{\lambda}, h_3 = 1$. Then, one can show

$$\begin{aligned} \dot{V} &\leq -\varepsilon \left(q - \frac{\lambda}{2\varepsilon} \right) \hat{u}^2(1, t) - \varepsilon \|\hat{u}_x[t]\|^2 + \varrho \|\hat{u}[t]\|^2 \\ &\quad + \frac{\varepsilon^2}{\lambda} (U_j^s)^2 + \left(\frac{\varepsilon^2 p_{10}^2}{\lambda} + \frac{1}{2} \right) \hat{u}^2(1, t), \end{aligned} \quad (49)$$

for $t \in (t_j^s, t_{j+1}^s), j \in \mathbb{N}$ where $\varrho > 0$ is given by (36). Using Cauchy Schwarz inequality and (11) under the consideration of (48), we can obtain that $(U_j^s)^2 \leq 2\|k\|^2 V(t_j^s)$. Thus, recalling Assumption 1 from which it follows that $q > \lambda/2\varepsilon$ for $\theta_1 = 0$, we can write (49) as

$$\dot{V} \leq 2\varrho V(t) + \frac{2\varepsilon^2 \|k\|^2}{\lambda} V(t_j^s) + \left(\frac{\varepsilon^2 p_{10}^2}{\lambda} + \frac{1}{2} \right) \hat{u}^2(1, t), \quad (50)$$

for $t \in (t_j^s, t_{j+1}^s), j \in \mathbb{N}$. Now let us find a known upper-bound for $|\hat{u}(1, t)|$. From Lemma 1 of [14], we can obtain that $\|\tilde{w}_x[t]\| \leq (\|\tilde{w}_x[0]\| + M_1 \|\tilde{w}[0]\|) e^{-\sigma^* t}$ and $\|\tilde{w}[t]\| \leq \|\tilde{w}[0]\| e^{-\sigma^* t}$ for all $t \geq 0$ where \tilde{w} is the observer error target state obtained via (9) with $\theta_1 = 0, \theta_2 = 1$ (see [14] for details), M_1 is given by (38), and σ^* is given by (36). Thus, using (8), Agmon's and Young's inequalities, we can obtain that

$$\begin{aligned} |\hat{u}(1, t)| &= |\tilde{w}(1, t)| \leq (\sqrt{2})^{-1} \|\tilde{w}[t]\| + (\sqrt{2})^{-1} \|\tilde{w}_x[t]\| \\ &\leq (\sqrt{2})^{-1} (M_1 + 1) \|\tilde{w}[0]\| e^{-\sigma^* t} + (\sqrt{2})^{-1} \|\tilde{w}_x[0]\| e^{-\sigma^* t}, \end{aligned} \quad (51)$$

for all $t \geq 0$. But, using (9) with $\theta_1 = 0, \theta_2 = 1$, and Cauchy-Schwarz inequality, we can show that $\|\tilde{w}[0]\| \leq \Omega_1 \|\tilde{u}[0]\|$ and $\|\tilde{w}_x[0]\| \leq \|\tilde{u}_x[0]\| + \Omega_2 \|\tilde{u}[0]\|$ where Ω_1 and Ω_2 are given by (39) and (40), respectively. Again using Cauchy-Schwarz inequality, we can obtain from (7) that $\|\tilde{u}[0]\| \leq \|u[0]\| + \|\hat{u}[0]\|$ and $\|\tilde{u}_x[0]\| \leq \|u_x[0]\| + \|\hat{u}_x[0]\|$. Thus, from (51), we can obtain the following bound for $\hat{u}^2(1, t)$

$$|\hat{u}(1, t)| \leq \Psi_0 e^{-\sigma^* t}, \quad (52)$$

for all $t \geq 0$ where $\Psi_0 = (\sqrt{2})^{-1} ((M_1 + 1)\Omega_1 + \Omega_2)\Psi_1 + (\sqrt{2})^{-1} \Psi_2 + (\sqrt{2})^{-1} ((M_1 + 1)\Omega_1 + \Omega_2) \|\hat{u}[0]\| +$

$(\sqrt{2})^{-1}\|\hat{u}_x[0]\|$. Then, considering (52) and noting that $e^{-2\sigma^*t} < e^{-2\sigma^*t_j^s}$ for all $t > t_j^s$, we obtain from (50) that

$$\dot{V}(t) \leq 2\rho V(t) + \frac{2\varepsilon^2\|k\|^2}{\lambda}V(t_j^s) + (\Psi_0^*)^2e^{-2\sigma^*t_j^s}, \quad (53)$$

for $t \in (t_j^s, t_{j+1}^s), j \in \mathbb{N}$ where Ψ_0^* is given by (37). Therefore, from (53), we can show that

$$V(t) \leq e^{2\rho(t-t_j^s)}V(t_j^s) + \frac{2\varepsilon^2\|k\|^2}{\lambda}V(t_j^s) + (\Psi_0^*)^2e^{-2\sigma^*t_j^s} (e^{2\rho(t-t_j^s)} - 1),$$

for $t \in [t_j^s, t_{j+1}^s), j \in \mathbb{N}$ from which we obtain that

$$\begin{aligned} & \|\hat{u}[t]\|^2 \\ & \leq \left(\|\hat{u}[t_j^s]\|^2 + \frac{\varepsilon^2\|k\|^2}{\lambda\rho} \|\hat{u}[t_j^s]\|^2 + \frac{(\Psi_0^*)^2e^{-2\sigma^*t_j^s}}{\rho} \right) e^{2\rho(t-t_j^s)}, \end{aligned} \quad (54)$$

considering (48). Using Cauchy Schwarz inequality and Young's inequality on (14), we can show that $d^2(t) \leq 2\|k\|^2\|\hat{u}[t_j^s]\|^2 + 2\|k\|^2\|\hat{u}[t]\|^2$. Then, using (54), we can obtain (46). Considering the dynamics of $m(t)$ given by (17) and the relation (46), we can show $\dot{m}(t) \geq -\eta m(t) - \rho H(t_j^s)e^{2\rho(t-t_j^s)}$ for $t \in (t_j^s, t_{j+1}^s), j \in \mathbb{N}$ from which we can obtain (47). This completes the proof of Lemma 3. ■

Now let us continue with the proof of Theorem 3. Consider the triggering function $\Gamma^c(t)$ given by (16) along the solution of (1)-(7),(11),(14),(17),(33)-(40). Further, let us assume that an event has occurred at $t = t_j^s$ and $m(t_j^s) > 0$. Then, as the control input is updated, it follows from (16) that $\Gamma^c(t_j^s) = -\gamma m(t_j^s) < 0$. Moreover, $\Gamma^c(t)$ will remain non-positive at least until $t = t_j^s + \tau$, where τ is the minimal dwell-time given by (25) (see R1 of Theorem 1). We have from (46) that $d^2(t) \leq H(t_j^s)e^{2\rho(t-t_j^s)}$ and from (47) that

$$\begin{aligned} \gamma m(t) & \geq \gamma m(t_j^s)e^{-\eta(t-t_j^s)} \\ & \quad - \frac{\gamma\rho H(t_j^s)}{2\rho + \eta} e^{-\eta(t-t_j^s)} (e^{(2\rho+\eta)(t-t_j^s)} - 1), \end{aligned}$$

for $t \in [t_j^s, t_{j+1}^s)$. Note that the RHS of (46) is an increasing function of t whereas the RHS of (47) is a decreasing function of t . Then, if there is a positive $t^\dagger > t_j^s$ that satisfies

$$\begin{aligned} H(t_j^s)e^{2\rho(t^\dagger-t_j^s)} & = \gamma m(t_j^s)e^{-\eta(t^\dagger-t_j^s)} \\ & \quad - \frac{\gamma\rho H(t_j^s)}{2\rho + \eta} e^{-\eta(t^\dagger-t_j^s)} (e^{(2\rho+\eta)(t^\dagger-t_j^s)} - 1), \end{aligned} \quad (55)$$

we can be certain that $d^2(t) \leq \gamma m(t)$, i.e., $\Gamma^c(t) \leq 0$ for $t \in [t_j^s, t^\dagger)$ (note that the LHS of (55) is an upper-bound for $d^2(t^\dagger)$, and the RHS of (55) is a lower-bound for $\gamma m(t^\dagger)$). Solving (55) for t^\dagger , we obtain that

$$t^\dagger = t_j^s + \frac{1}{2\rho + \eta} \ln \left(\frac{\gamma m(t_j^s) + \frac{\gamma\rho H(t_j^s)}{2\rho + \eta}}{H(t_j^s) + \frac{\gamma\rho H(t_j^s)}{2\rho + \eta}} \right).$$

If $t^\dagger > t_j^s + \tau$, the next event can be chosen as $t_{j+1}^s = t^\dagger$. If $t^\dagger \leq t_j^s + \tau$, the next event can be chosen as $t_{j+1}^s = t_j^s + \tau$. In this way, since the next event time is given by (33)-(40), it is

ensured that $\Gamma^c(t) \leq 0$ for $t \in [t_j^s, t_{j+1}^s)$ while preventing the occurrence of Zeno phenomenon. Then, employing the same line of reasoning as in the proof of Theorem 2, we can show that $\Gamma^c(t) \leq 0$ for all $t \in [t_j^s, t_{j+1}^s), j \in \mathbb{N}$ and $m(t) > 0$ for all $t > 0$. Thus, the L^2 -exponential convergence to zero satisfying the estimate (28) follows from R4 of Theorem 1. This completes the proof of Theorem 3. ■

REFERENCES

- [1] A. Anta and P. Tabuada, "To sample or not to sample: Self-triggered control for nonlinear systems," *IEEE Transactions on automatic control*, vol. 55, no. 9, pp. 2030–2042, 2010.
- [2] D. P. Borgers, R. Postoyan, A. Anta, P. Tabuada, D. Nešić, and W. Heemels, "Periodic event-triggered control of nonlinear systems using overapproximation techniques," *Automatica*, vol. 94, pp. 81–87, 2018.
- [3] M. Diagne and I. Karafyllis, "Event-triggered boundary control of a continuum model of highly re-entrant manufacturing systems," *Automatica*, vol. 134, p. 109902, 2021.
- [4] N. Espitia, "Observer-based event-triggered boundary control of a linear 2×2 hyperbolic systems," *Systems & Control Letters*, vol. 138, p. 104668, 2020.
- [5] N. Espitia, I. Karafyllis, and M. Krstic, "Event-triggered boundary control of constant-parameter reaction-diffusion PDEs: a small-gain approach," *Automatica*, vol. 128, p. 109562, 2021.
- [6] W. H. Heemels, M. Donkers, and A. R. Teel, "Periodic event-triggered control for linear systems," *IEEE Transactions on automatic control*, vol. 58, no. 4, pp. 847–861, 2012.
- [7] W. Heemels and M. Donkers, "Model-based periodic event-triggered control for linear systems," *Automatica*, vol. 49, no. 3, pp. 698–711, 2013.
- [8] W. Heemels, K. H. Johansson, and P. Tabuada, "An introduction to event-triggered and self-triggered control," in *2012 51st IEEE Conference on Decision and Control (CDC)*. IEEE, 2012, pp. 3270–3285.
- [9] R. Katz, E. Fridman, and A. Selivanov, "Boundary delayed observer-controller design for reaction-diffusion systems," *IEEE Transactions on Automatic Control*, 2020.
- [10] M. Mazo, A. Anta, and P. Tabuada, "On self-triggered control for linear systems: Guarantees and complexity," in *2009 European Control Conference (ECC)*. IEEE, 2009, pp. 3767–3772.
- [11] B. Rathnayake and M. Diagne, "Observer-based event-triggered boundary control of the one-phase Stefan problem," *arXiv preprint arXiv:2210.00412*, 2022.
- [12] —, "Periodic event-triggered boundary control of a class of reaction-diffusion PDEs," in *2023 American Control Conference (ACC)*. IEEE, 2023, pp. 1800–1806.
- [13] B. Rathnayake, M. Diagne, N. Espitia, and I. Karafyllis, "Observer-based event-triggered boundary control of a class of reaction-diffusion PDEs," *IEEE Transactions on Automatic Control*, vol. 67, no. 6, pp. 2905–2917, 2021.
- [14] B. Rathnayake, M. Diagne, and I. Karafyllis, "Sampled-data and event-triggered boundary control of a class of reaction-diffusion PDEs with collocated sensing and actuation," *Automatica*, vol. 137, p. 110026, 2022.
- [15] M. Wakaiki and H. Sano, "Stability analysis of infinite-dimensional event-triggered and self-triggered control systems with Lipschitz perturbations," *arXiv preprint arXiv:1911.12916*, 2019.
- [16] —, "Event-triggered control of infinite-dimensional systems," *SIAM Journal on Control and Optimization*, vol. 58, no. 2, pp. 605–635, 2020.
- [17] H. Wan, X. Luan, H. R. Karimi, and F. Liu, "Dynamic self-triggered controller codesign for Markov jump systems," *IEEE Transactions on Automatic Control*, vol. 66, no. 3, pp. 1353–1360, 2020.
- [18] J. Wang and M. Krstic, "Event-triggered adaptive control of a parabolic PDE-ODE cascade with piecewise-constant inputs and identification," *IEEE Transactions on Automatic Control*, 2022.
- [19] W. Wang, R. Postoyan, D. Nešić, and W. Heemels, "Periodic event-triggered control for nonlinear networked control systems," *IEEE Transactions on Automatic Control*, vol. 65, no. 2, pp. 620–635, 2019.
- [20] X. Yi, K. Liu, D. V. Dimarogonas, and K. H. Johansson, "Dynamic event-triggered and self-triggered control for multi-agent systems," *IEEE Transactions on Automatic Control*, vol. 64, no. 8, pp. 3300–3307, 2018.